Molecular structure and conformation of diethylmethylamine determined by gas electron diffraction and vibrational spectroscopy combined with theoretical calculations

Hiroshi Takeuchi,* Masaki Ito, Toru Egawa

Division of Chemistry, Graduate School of Science, Hokkaido University, Sapporo 060-0810, Japan

* Corresponding author. Tel: +81-11-706-3533. Fax: +81-11-706-4924.

E-mail: takehi@sci.hokudai.ac.jp

Abstract

We have investigated the molecular structure and conformation of diethylmethylamine, C(4)H_3C(2)H_2N(1)[CH_3]C(3)H_2C(5)H_3, by gas electron diffraction and vibrational spectroscopy with the aid of theoretical calculations. Diffraction data are consistent with a conformational mixture of 35(14)% tt + 27(14)% g^+t + 20(17)% g^-t + 18(23)% g^+g^+ where the numbers in parentheses denote three times the standard errors (3σ). Normal-coordinate analysis based on B3LYP/6-311+G^{**} calculations supports the existence of the four conformers. The dihedral angle ϕ_1(C4C2N1C3) (= $-\phi_2$(C5C3N1C2)) of the tt conformer was 170(4)º whereas the ϕ_1 and ϕ_2 values of the other conformers were fixed at the B3LYP/6-311++G(2df,p) values: 72.4º and –163.3º for the g^+t, –66.0º and –158.2º for the g^-t, and 60.3º and 63.5º for the g^+g^+. Average values of the structural parameters (r_g/Å and $\angle_\alpha$/º) with 3σ are: <r(N–C)> = 1.462(2),

<r(C–C)> = 1.523(3), <r(C–H)> = 1.113(2), <∠CNC> = 111.6(5), <∠NCC> = 114.5(5), <∠NCH/∠CCH_{Me}> = 110.6(5).

Keywords: Diethylmethylamine; molecular structure; conformation; electron diffraction; vibrational spectroscopy.

1. Introduction

Amines with at least one ethyl group exhibit conformational flexibility. To understand it, gas-phase molecular structures and conformations of ethylamine [1], methylethylamine [2, 3] and dimethylethylamine [4-6] have been investigated by spectroscopic and diffraction methods. These studies indicate that the *trans* CNCC conformer is preferred to the g*auche* conformer. For more complicated amines with ethyl groups, diethylamine, triethylamine and *N*-chloro-*N*-ethylethanamine (Et_2NCl), we have determined their molecular structures and conformations by gas electron diffraction (GED) combined with ab initio calculations [7, 8]. Two or more conformers were detected for each compound. In the present study, we have determined the molecular structure and conformation of diethylmethylamine (DEMA) by GED. The obtained results are compared with conformations of related amines.

Bushweller et al. [9] investigated conformation of DEMA by ^{1}H NMR spectroscopy with the aid of empirical force-field calculations. ^{1}H NMR spectra of DEMA, $(CH_3CD_2)_2NCH_3$ and $(CD_3CH_2)_2NCH_3$ were recorded in $CBrF_3$ solution at temperatures of 100 K to 200 K. Each of spectra measured at about 100 K was decomposed into two subspectra consisting of some lines. The authors assigned the major and minor subspectra (85% and 15%) to tt/g^+t and g^-t/g^+g^+ families (see Fig. 1), respectively. In

each family, conformation is easily converted.

IR and Raman spectra of DEMA in the solid, liquid and gas phases were studied by Crocker and Goggin [6]. Two conformers detected in the solid phase were suggested to be tt and g^+t. On the other hand, from the complexity of a vapor spectrum, they concluded that two or more conformers exist in the gas phase. Therefore, conformational analysis of DEMA is an open problem.

A few vibrational frequencies relating to N-C stretching modes are reported by Crocker and Goggin [6] and IR spectra of the liquid are available from Ref. [10]. To perform vibrational and conformational analysis in more details, gas-phase IR spectra and FT-Raman spectra of the liquid have been measured in the present study. Furthermore, RHF, MP2 [11] and B3LYP [12, 13] calculations with various basis sets are carried out to obtain information on the structure, conformation and force field of DEMA. Since the B3LYP/6-311+G** calculations with wavenumber-linear scale factors provide reasonable estimate of vibrational frequencies [14], the density functional theory calculations at the same level are used to interpret vibrational spectra. Structural constraints in GED analysis are taken from results of B3LYP calculations with a larger basis set 6-311++G(2df,p).

2. Experimental

A commercial sample of DEMA (Aldrich) with a purity of 98% was used after distillation in vacuum. The experiments were made with an apparatus equipped with an r^3-sector [15] at two camera distances, 245.1 mm (short) and 490.2 mm (long). Diffraction patterns were recorded on 8 × 8 in. Kodak projector slide plates at room temperature (24°C). The accelerating voltage was about 37 kV. The diffraction

patterns of carbon disulfide were recorded after those of DEMA to determine the wavelength of incident electrons (r_a(C–S) = 1.5570 Å) [16]. The plates were developed in Kodak Dektol developer diluted 1:1 for 4.5 min. Other experimental conditions are as follows: exposure times, 92 s (short) and 47 s (long); electron wavelengths, 0.06348 Å (short) and 0.06373 Å (long); sample pressure, 35 Torr; beam current, 2.4 μA; uncertainties of scale factor, 0.04%.

Optical densities were measured with a microphotometer of double-beam autobalanced type. The average densities obtained at intervals of 0.5 mm were converted to total intensities [17], which were then divided by theoretical backgrounds to level total intensities. The leveled total intensities were obtained from four and two plates for short- and long-camera distances, respectively. They were averaged and used for data analysis. Elastic and inelastic scattering factors were taken from Ref. [18]. The leveled total intensities are deposited as supplementary data. The molecular scattering intensities and experimental radial distribution curve of DEMA are shown in Figs. 2 and 3, respectively.

Gas-phase IR spectra were measured at resolutions of 0.5 cm^{-1} by using a BOMEM DA 3.16 Fourier transform spectrometer at room temperature. In the measurement, a cell with KBr windows and a path of 10 cm was used. The FT-Raman spectra of liquid DEMA were recorded on the same spectrometer at 4 cm^{-1} resolution by using an Nd:YAG laser. No impurity was detected in these spectroscopic measurements.

3. Structural Determination

3.1. Theoretical calculations

Calculations were carried out using Gaussian 98 [19]. Geometries of the five

conformers shown in Fig. 1 and g^+g^- conformer were optimized at the HF/6-31G** level with no symmetry restriction. The g^+g^- form converged to tg^- form, the mirror image of g^+t. Therefore, for the five conformers except the g^+g^- conformer, further geometry optimization was carried out by MP2 [11] and B3LYP [12, 13] methods. MP2 calculations were performed with frozen-core approximation using 6-31G** and 6-311+G** basis sets. For B3LYP method, we used three kinds of basis sets, 6-31G**, 6-311+G** and 6-311++G(2df,p). Table 1 shows that relative energies of these conformers depend on the calculation method and basis set, whereas the order of the stability is consistent through all the calculations. The structures optimized at B3LYP/6-311++G(2df,p) level are listed in Table 2.

The populations of the tt, g^+t, g^-t, g^+g^+ and g^-g^+ conformers were estimated from the energy differences listed in Table 1. All the calculations suggest that the population of g^-g^+ form is negligibly small (≤ 0.5%). This is consistent with the results of vibrational analysis described in next section.

3.2. Vibrational analysis

Cartesian force constants of the five conformers were obtained from the B3LYP/6-311+G** calculations using Gaussian 98 [19] and were transformed into the quadratic force constants of local symmetry coordinates $f_{ij}^{\text{B3LYP/6-311+G**}}$. The force constants were furthermore modified by using the equation of $f_{ij}^{\text{scaled}} = (c_i c_j)^{1/2} f_{ij}^{\text{B3LYP/6-311+G**}}$ [20] where c_i's denote scale factors for force constants. Scale factors were derived by referring to wavenumber-linear scale factors reported in [14]: c_i's were 0.9197 for C-H stretching coordinates whereas c_i's for other coordinates were 0.9841. The scaled force constants were used to calculate mean amplitudes and

shrinkage corrections, $r_\alpha - r_a$, [21] required for the analysis of GED data.

Table 3 compares observed vibrational wavenumbers with calculated ones in the range of 1250 to 400 cm^{-1} which is useful to investigate conformation of DEMA. Three bands at about 773, 762 and 749 cm^{-1} observed in the gas and liquid phases are unambiguously assigned to the tt, g^+t and g^-t conformers, respectively. The existence of the g^+g^+ form in the gas phase is uncertain since no bands can be assigned solely to this form. However, Table 1 suggests that the stability of this form is similar to that of the g^-t form. Therefore, the g^+g^+ conformer seems to be present in the gas phase. On the other hand, the Raman and IR spectra of the liquid show the bands at 408 and 978 cm^{-1}, which are assigned to the g^+g^+ conformer. Therefore, the vibrational bands in the liquid phase are apparently interpreted in terms of coexistence of the four conformers.

3.3. Analysis of gas electron diffraction data

The following assumptions were made: (1) The model consisting of the tt, g^+t, g^-t and g^+g^+ conformers were adopted and the result is discussed later. (2) The N–C, C–C and C–H bond lengths, and CNC and NCC bond angles were refined in groups and differences in each group were fixed at the differences derived from B3LYP/6-311++G(2df,p) calculations. (3) The NCH and CCH_{Me} bond angles were refined in one group and differences in the group were taken from B3LYP/6-311++G(2df,p) calculations. (4) The NCCH, C2NC3H, C2NC6H, C3NC2H, C3NC2C4 (ϕ_1) and C2NC3C5 (ϕ_2) dihedral angles were fixed at B3LYP/6-311++G(2df,p) values except for ϕ_1 and ϕ_2 of the tt conformer. The dihedral angles around the N-C_{Et} bonds of this conformer were refined by assuming the C_s symmetry ($\phi_1 = -\phi_2$). (5) Mean amplitudes were refined in four groups as shown in

Table 4. Groups were separated at 1.8, 2.8 and 3.55 Å so that each group corresponds to one or more separated peaks of the experimental radial distribution curve (Fig. 3). The differences in each group were fixed at the calculated values. (6) Asymmetry parameters were estimated by the conventional methods [22].

Adjustable structural parameters, r(N–C), r(C–C), r(C–H), ∠CNC, ∠NCC, ∠NCH and ϕ_1(tt), abundances of conformers, X(tt), X(g$^+$t) and X(g$^-$t), mean amplitudes l_1 - l_4 and indices of resolution for long- and short-camera distances, k_l and k_s, were determined by the least-squares calculations on molecular scattering intensities. There are no significant differences between refined and calculated mean amplitudes as shown in footnote of Table 4. Table 5 lists the structural parameters and conformational composition of DEMA obtained by GED. Correlation matrix elements [23] with absolute values larger than 0.6 are: X(tt)/X(g$^+$t) = –0.61, <r(N–C)>/<r(C–C)> = –0.83, <r(N–C)>/l_1 = 0.62, <r(C–C)>/l_1 = –0.62.

The mean amplitudes were calculated from the scaled force constants using the small-amplitude vibrational model. The validity of the model and force field used in this work can be roughly evaluated by comparing the calculated amplitudes with those obtained from GED data. The differences between the calculated and observed amplitudes are comparable to three times the standard errors (see Table 4), suggesting that the small-amplitude model and the scaled force field are reasonable for DEMA.

4. Discussion

Fig. 3 shows differences between the experimental radial distribution curve and the curves calculated by assuming one-conformer model. These differences indicate that any model consisting of one conformer is not acceptable. The conformational

composition of DEMA was determined by GED to be 35(14)% tt + 27(14)% g^+t + 20(17)% g^-t + 18(23)% g^+g^+ with the *R*-factor of 0.039 (see the footnote *a* of Table 5 for the definition). The value is much smaller than those of one-conformer models, 0.086 (tt), 0.078 (g^+t), 0.105 (g^-t) and 0.098 (g^+g^+). GED could not identify the existence of the g^+g^+ conformer with certainty. By taking into account the multiplicity of the tt, g^+t, g^-t and g^+g^+ conformers (1, 2, 2 and 2, respectively), it is found that the tt conformer is the most stable.

To examine the dependence of the experimental results on theoretical constraints included in the assumptions, the B3LYP/6-311++G(2df,p) constraints were compared with the corresponding values derived from the structures at the other levels of theory, which are deposited as supplementary data. Large differences were found for the MP2/6-311+G** values of ϕ_2 of the g^+t, g^-t and g^+g^+ conformers: these values (-174.2, -164.5 and 57.9°) are smaller than the B3LYP/6-311++G(2df,p) values by 10.0, 6.3 and 5.6°, respectively, whereas the remaining values of ϕ_1 and ϕ_2 are equal to the B3LYP/6-311++G(2df,p) values within 5°. The analysis where ϕ_1 and ϕ_2 of the g^+t, g^-t and g^+g^+ conformers were fixed at the MP2/6-311+G** values resulted in the conformational composition close to the above result: 38% tt + 23% g^+t + 18% g^-t + 21% g^+g^+ with the *R*-factor of 0.039. Therefore, the constraints from the theoretical calculations do not significantly affect the experimental results.

Table 3 shows that the vibrational bands of the liquid are assigned to the four conformers. Vibrational analysis of the hydrocarbon analogue, 3-methylpentane, in the liquid phase identifies the conformers corresponding to the tt, g^+t, g^-t and g^+g^+ of DEMA [24, 25]. Crocker and Goggin [6] suggested that two bands in the IR and Raman spectra of the solid DEMA, 776 and 762 cm^{-1}, were assigned to two conformers,

tt and g^+t. In the present study, the assignments were confirmed by the vibrational analysis aided with the B3LYP/6-311+G^{**} calculations. The above discussion on conformational analysis of DEMA indicates that the tt and g^+t conformers are more stable than the g^-t and g^+g^+ conformers. The conformational stability of DEMA can be explained in terms of the number of *trans* CNCC fragments as follows: Two CNCC fragments of the tt and g^+t conformers take *trans* conformation whereas one fragment is *trans* for the g^-t and g^+g^+ conformers.

In diethylamine [7], tt and g^+t forms exist exclusively (42(16)% tt + 53(24)% g^+t + 5(20)% g^+g^+) and the former is more stable than the latter. The g^-t form is not detected in diethylamine. The difference in diethylamine and DEMA indicates that steric interaction between C6-methyl and ethyl groups is an important factor determining conformational stability of DEMA.

For *N*-chloro-*N*-ethylethanamine [8], the tt and g^+t conformers exist with the populations of 68(8)% and 32(8)%, respectively. It is well known that a methyl group has nearly the same size as a chlorine atom. Therefore, it may not be justified to ascribe the absence of g^-t and g^+g^+ conformers in gaseous *N*-chloro-*N*-ethylethanamine to the steric repulsion and more feasible explanation seems to be possible by means of the electronegativity of Cl. The substitution of the chlorine atom by the methyl group decreases the stability of the tt and g^+t conformers relative to the g^-t and g^+g^+ conformers.

Our study on triethylamine [7] shows that CCNCC moieties take tt, g^+t, g^-t and g^+g^+ conformations. Therefore, the g^-g^+ conformation is not observed in diethylamine, DEMA and triethylamine. This is ascribable to steric repulsion between terminal methyl groups in the g^-g^+ conformation.

Acknowledgments

We thank the Computer Center, Institute for Molecular Science, Okazaki National Research Institutes, for the use of the NEC HPC and Fujitsu VPP5000 computers and GAUSSIAN 98. Numerical computations were carried out on a Hitachi Model MP5800/160 at the Hokkaido University Computing Center.

Supplementary data

Supplementary data associated with this article (tables of the leveled total intensities and the backgrounds, and the structures derived from the HF/6-31G**, MP2/6-31G**, MP2/6-311+G**, B3LYP/6-31G** and B3LYP/6-311+G** calculations) can be found in the online version.

References

[1] Y. Hamada, M. Tsuboi, K. Yamanouchi, K. Kuchitsu, J. Mol. Struct. 146 (1986) 253.

[2] J. R. Durig, D. A. C. Compton, J. Phys. Chem. 83 (1979) 2873.

[3] G. Gamer, H. Wolff, Spectrochim. Acta, 29A (1973) 129.

[4] J. H. M. ter Brake, V. Mom, F. C. Mijlhoff, J. Mol. Struct. 65 (1980) 303.

[5] J. R. Durig, F. O. Cox, J. Mol. Struct. 95 (1982) 85.

[6] C. Crocker. P. L. Goggin, J. Chem. Soc. Dalton Trans. (1978) 388.

[7] H. Takeuchi, T. Kojima, T. Egawa, S. Konaka, J. Phys. Chem. 96 (1992) 4389.

[8] N. Kuze, H. Takeuchi, T. Egawa, S. Konaka, S. Q. Newton, L. Schäfer, J. Mol. Struct., 291 (1993) 11.

[9] C. H. Bushweller, S. H. Fleischman, G. L. Grady, P. McGoff, C. D. Rithner, M. R. Whalon, J. G. Brennan, R. P. Marcantonio, R. P. Domingue, J. Am. Chem. Soc. 104 (1982) 6224.

[10] SDBSWeb: http://www.aist.go.jp/RIODB/SDBS/ (National Institute of Advanced Industrial Science and Technology, 1993).

[11] C. Møller, M. S. Plesset, Phys. Rev. 46 (1934) 618.

[12] A. D. Becke, J. Chem. Phys. 98 (1993) 5648.

[13] C. Lee, W. Yang, R.G. Parr, Phys. Rev. B37 (1988) 785.

[14] H. Yoshida, A. Ehara, H. Matsuura, Chem. Phys. Lett. 325 (2000) 477.

[15] S. Konaka, M. Kimura, 13th Austin Symposium on Gas Phase Molecular Structure, The University of Texas, Austin, TX, 12-14 March 1990, S21.

[16] A. Tsuboyama, A. Murayama, S. Konaka, M. Kimura, J. Mol. Struct. 118 (1984) 351.

[17] H. Takeuchi, J. Enmi, M. Onozaki, T. Egawa, S. Konaka, J. Phys. Chem. 98 (1994) 8632.

[18]. A.W. Ross, M. Fink and R. Hilderbrandt, J. Wang, V. H. Smith Jr. in: A.J.C. Wilson (Ed.), International Tables for X-Ray Crystallography, Kluwer Academic Publishers, Dordrecht, Boston and London, 1995 Vol. C, p. 245.

[19] M. J. Frisch, G. W. Trucks, H. B. Schlegel, G. E. Scuseria, M. A. Robb, J. R. Cheeseman, V. G. Zakrzewski, J. A. Montgomery Jr., R. E. Stratmann, J. C. Burant, S. Dapprich, J. M. Millam, A. D. Daniels, K. N. Kudin, M. C. Strain, O. Farkas, J. Tomasi, V. Barone, M. Cossi, R. Cammi, B. Mennucci, C. Pomelli, C. Adamo, S. Clifford, J. Ochterski, G. A. Petersson, P. Y. Ayala, Q. Cui, K. Morokuma, D. K. Malick, A. D. Rabuck, K. Raghavachari, J. B. Foresman, J. Cioslowski, J. V. Ortiz, A. G. Baboul, B. B. Stefanov, G. Liu, A. Liashenko, P. Piskorz, I. Komaromi, R. Gomperts, R. L. Martin, D. J. Fox, T. Keith, M. A. Al-Laham, C. Y. Peng, A. Nanayakkara, M. Challacombe, P. M. W. Gill, B. Johnson, W. Chen, M. W. Wong, J. L. Andres, C. Gonzalez, M. Head-Gordon, E. S. Replogle, J. A. Pople, Gaussian 98 (Revision A.9), Gaussian Inc., Pittsburgh, PA, 1998.

[20] J. E. Boggs, in I. Hargittai, M. Hargittai (Eds.). Stereochemical Applications of Gas-phase Electron Diffraction, VCH, New York, 1988 Part B, Ch. 10.

[21] K. Kuchitsu, S. J. Cyvin, in S. J. Cyvin (Ed.). Molecular Structures and Vibrations, Elsevier, Amsterdam, 1972, Ch. 12.

[22] K. Kuchitsu, L. S. Bartell, J. Chem. Phys. 35 (1961) 1945.

[23] I. Hargittai, in I. Hargittai, M. Hargittai (Eds.), Stereochemical Applications of Gas-phase Electron Diffraction, VCH, New York, 1988 Part A, Ch. 1.

[24] G. A. Crowder, D. Hill, J. Mol. Struct. 145 (1986) 69.

[25] N. G. Mirkin, S. Krimm, J. Mol. Struct. 550-551 (2000) 67.

Table 1

Calculated relative energies and populations of five conformers of diethylmethylamine

	Relative energy / kJ mol^{-1}					Population / %				
	tt[a]	g^+t	g^-t	g^+g^+	g^-g^+	tt	g^+t	g^-t	g^+g^+	g^-g^+
RHF/6-31G**	0.0	0.2	1.8	2.9	10.7	22.4	41.2	22.0	14.1	0.3
MP2/6-31G**	0.0	0.5	2.5	2.5	12.6	24.5	40.1	17.7	17.5	0.1
MP2/6-311+G**	0.0	0.6	4.7	3.9	15.6	30.4	47.6	9.2	12.8	0.1
B3LYP/6-31G**	0.0	0.6	2.8	3.5	9.9	26.9	42.1	17.4	13.1	0.5
B3LYP/6-311+G**	0.0	0.5	4.3	4.9	12.4	30.7	49.6	11.0	8.6	0.2
B3LYP/6-311++G(2df, p)	0.0	0.6	4.4	5.1	12.6	31.3	50.0	10.5	8.0	0.2

[a]Total energies of RHF/6-31G**, MP2/6-31G**, MP2/6-311+G**, B3LYP/6-31G**, B3LYP/6-311+G** and B3LYP/6-311++G(2df,p) calculations are -251.35802 E_h, -252.26771 E_h, -252.36227 E_h, -253.12006 E_h, -253.17728 E_h and -253.18745 E_h, respectively.

Table 2

Bond lengths (Å), bond angles and dihedral angles (°) of diethylmethylamine calculated at the B3LYP/6-311++G(2df,p) level

parameter [a]	tt	g^+t	g^-t	g^+g^+	g^-g^+
r(N1–C2)	1.463	1.464	1.462	1.460	1.454
r(N1–C3)	1.463	1.463	1.460	1.463	1.454
r(N1–C6)	1.455	1.455	1.453	1.453	1.447
r(C2–C4)	1.525	1.525	1.536	1.525	1.539
r(C3–C5)	1.525	1.526	1.527	1.537	1.539
∠C2N1C3	111.4	112.6	113.9	115.7	118.3
∠C2N1C6	112.1	111.0	113.4	111.9	115.7
∠C3N1C6	112.1	112.0	113.7	113.3	115.7
∠N1C2C4	113.9	113.9	117.2	113.9	118.3
∠N1C3C5	113.9	113.8	113.3	117.1	118.3
ϕ(C3N1C2C4)	165.3	72.4	–66.0	60.3	–81.0
ϕ(C6N1C2C4)	–68.2	–161.2	66.1	–167.9	62.9
ϕ(C2N1C3C5)	–165.3	–163.3	–158.2	63.5	80.7
ϕ(C6N1C3C5)	68.2	70.7	69.8	–67.6	–63.2

[a]The structural parameters including hydrogen atoms are omitted for simplicity.

Table 3

Observed and calculated wavenumbers (cm^{-1}) and potential energy distributions (PED) for diethylmethylamine[a]

Obs			Calc	PED(%)
IR[b] Gas	Raman[b] liquid	IR[c] liquid		
1244sh			1252, 1253	g^+t[b(27)], g^-t[b(21)]
1239m			1245	tt[b(27)]
1232m		1235	1233	tt[S(22),b(22),P(21)]
1227m		1227	1230	g^-t[P(26),b(23)]
1218sh		1221	1225	g^+t[P(23),S(22),b(22)]
		1217	1223	g^+g^+[P(29),b(24)]
1208m		1207		
1166sh			1169	g^+t[b(55),P(22)]
1160m		1156	1165, 1159	tt[b(52)], g^+g^+[b(58)]
1149sh			1149	g^-t[b(58)]
			1117, 1113	tt[P(33),b(30)], g^+g^+[b(61)]
1110sh			1110	g^+t[b(51)]
1104sh			1106, 1107	tt[b(52)],g^-t[b(50)]
1098m		1100	1099	g^+t[b(36)]
1094sh		1094	1096	g^-t[b(40)]
1085sh			1090, 1091	g^-t[b(31)], g^+g^+[b(37)]

1070s			1077, 1076, 1077	tt[b(56)], g^+t[b(45)], g^+g^+[b(43),S(26)]
1065s	1067m	1064	1071, 1069, 1071	tt[R(48)], g^+t[b(26),S(22)], g^+g^+[b(27),R(21)]
1060s	1059sh	1058	1060, 1061	g^+t[R(28),b(28)], g^-t[R(37)]
1049m		1047	1047	tt[R(40),b(30)]
			1040, 1035	g^+g^+[R(42)], g^-t[R(29),b(21)]
994m		992	992, 993	tt[S(33),b(32)], g^+t[R(46),S(26)]
		978	973	g^+g^+[R(55)]
		970	967	g^-t[R(47),S(21)]
908w	909w	910	910, 909	tt[R(44)], g^+t[b(30)]
			893, 891	g^-t[R(35),b(24)], g^+g^+[R(31),b(31)]
811w		808	813, 811, 808	tt[b(53),P(51)], g^+g^+[b(53),P(49)], g^+t[P(53),b(51)]
			803, 805	g^+t[P(55),b(51)], g^-t[P(56),b(52)]
			798	tt[P(61),b(50)]
			782, 779	g^-t[P(54),b(51)], g^+g^+[P(60),b(52)]
773m	774m	776	773	tt[S(76),b(24)]
762m	760m	761	759	g^+t[S(70),b(22)]
749sh	747m	750	750	g^-t[S(75)]
			743	g^+g^+[S(63)]
			525	g^-t[X(59),b(22),Y(21)]
	494w	491	486, 484, 488	tt[X(62),Y(44)], g^+t[X(51),Y(34)], g^+g^+[Y(39),X(57)]
			474	g^+g^+[Y(45),X(38)]
	458s		450	g^+t[Y(40),X(32)]

434s	426, 423	tt[Y(31),X(26)], g^{-}t[Y(78)]
408w	413	$g^{+}g^{+}$[Y(60)]

[a]Wavenumbers between 1250 and 400 cm^{-1} are listed. Abbreviations used: s, strong; m, medium; w, weak; sh, shoulder; R, C–C stretching; S, N–C stretching; b, methyl rocking; P, methylene rocking; X, NCC bending; Y, CNC bending. Contributions less than 20% were omitted. Calculated wavenumbers lower than 400 cm^{-1} are 384, 356, 270, 247, 203, 195, 81 and 77 cm^{-1} for tt, 397, 314, 287, 232, 218, 204, 100 and 70 cm^{-1} for g^{+}t, 394, 330, 265, 228, 210, 203, 98 and 85 cm^{-1} for g^{-}t, and 297, 285, 241, 224, 213, 133 and 76 cm^{-1} for $g^{+}g^{+}$, respectively. Calculated wavenumbers of $g^{-}g^{+}$ form are: 1239, 1137, 1105, 1100, 1091, 1056, 1039, 950, 879, 791, 774, 731, 494, 444, 418, 312, 233, 232, 216, 197, 110 and 52 cm^{-1}.

[b]Present study.

[c]Taken from the literature [6, 10].

Table 4

Mean amplitudes l_{ij} and interatomic distances r_a of diethylmethylamine (Å)

Atom pair[a]	tt			g^+t			g^-t			g^+g^+		
	l_{ij}^{obs}	r_a	n[b]	l_{ij}^{obs}	r_a	n[b]	l_{ij}^{obs}	r_a	n[b]	l_{ij}^{obs}	r_a	n[b]
<C–H>	0.083	1.107	1	0.083	1.107	1	0.083	1.107	1	0.083	1.107	1
<N–C>	0.054	1.460	1	0.054	1.461	1	0.054	1.458	1	0.054	1.459	1
<C–C>	0.055	1.519	1	0.055	1.519	1	0.057	1.525	1	0.056	1.525	1
C2···C3	0.076	2.404	2	0.075	2.420	2	0.073	2.434	2	0.072	2.460	2
C2···C6	0.075	2.404	2	0.077	2.390	2	0.073	2.420	2	0.076	2.398	2
C3···C6	0.075	2.404	2	0.074	2.403	2	0.075	2.424	2	0.073	2.420	2
N1···C4	0.074	2.490	2	0.075	2.492	2	0.075	2.549	2	0.075	2.549	2
N1···C5	0.074	2.490	2	0.074	2.484	2	0.074	2.480	2	0.074	2.491	2
C2···C5	0.087	3.755	4	0.090	3.749	4	0.092	3.745	4	0.122	3.105	3
C3···C4	0.087	3.755	4	0.115	3.072	3	0.130	3.094	3	0.111	3.009	3
C4···C5	0.127	4.932	4	0.176	4.271	4	0.143	4.561	4	0.280	3.727	4
C4···C6	0.130	2.991	3	0.090	3.732	4	0.125	3.053	3	0.084	3.755	4
C5···C6	0.130	2.991	3	0.130	3.054	3	0.125	3.073	3	0.122	3.064	3

[a]The mean amplitudes of relatively important atom pairs are listed. The bracket denotes an average value.

[b]The mean amplitudes with the same number were refined as one group. Values of $l_{ij}^{obs} - l_{ij}^{calc}$ are 0.004(2), 0.005(3), −0.012(9) and 0.011(9) Å for groups 1, 2 3, and 4,

respectively, where the numbers in parentheses are three times the standard errors from the least-squares refinement 3σ.

Table 5

Structural parameters and conformational composition of diethylmethylamine[a]

Parameters	tt	g^+t	g^-t	g^+g^+
r_g(N1–C2)	1.465(2), r_1[b]	1.466(r_1)[c]	1.464(r_1)[c]	1.462(r_1)[c]
r_g(N1–C3)	1.465(r_1)[c]	1.465(r_1)[c]	1.462(r_1)[c]	1.465(r_1)[c]
r_g(N1–C6)	1.457(r_1)[c]	1.457(r_1)[c]	1.455(r_1)[c]	1.455(r_1)[c]
r_g(C2–C4)	1.521(3) , r_2[b]	1.521(r_2)[c]	1.532(r_2)[c]	1.521(r_2)[c]
r_g(C3–C5)	1.521(r_2)[c]	1.522(r_2)[c]	1.523(r_2)[c]	1.533(r_2)[c]
$\angle_\alpha$C2N1C3	110.5(5), θ_1[b]	111.7(θ_1)[c]	113.0(θ_1)[c]	114.8(θ_1)[c]
$\angle_\alpha$C2N1C6	111.2(θ_1)[c]	110.1(θ_1)[c]	112.5(θ_1)[c]	111.0(θ_1)[c]
$\angle_\alpha$C3N1C6	111.2(θ_1)[c]	111.1(θ_1)[c]	112.8(θ_1)[c]	112.4(θ_1)[c]
$\angle_\alpha$N1C2C4	114.0(5), θ_2[b]	114.0(θ_2)[c]	117.3(θ_2)[c]	114.0(θ_2)[c]
$\angle_\alpha$N1C3C5	114.0(θ_2)[c]	113.9(θ_2)[c]	113.4(θ_2)[c]	117.2(θ_2)[c]
ϕ_1(C3N1C2C4)	170(4)	72.4[e]	–66.0[e]	60.3[e]
ϕ_2(C2N1C3C5)	–170[d]	–163.3[e]	–158.2[e]	63.5[e]
Abundance/%	35(14)	27(14)	20(17)	18(23)

[a]Bond lengths in Å and angles in degrees. The structural parameters averaged over the conformers are: <r(N–C)> = 1.462(2), <r(C–C)> = 1.523(3), <r(C–H)> = 1.113(2), <∠CNC> = 111.6(5), <∠NCC> = 114.5(5), <∠NCH/∠CCH_{Me}> = 110.6(5), where < > denotes an average value. The numbers in parentheses are 3σ, where σ denotes the standard error from the least-squares refinement. Indices of resolutions for short- and

long-camera distances are 0.92(1) and 0.92(2), respectively. The *R*-factor defined by the equation of $R = \{\Sigma_i W_i(sM(s)_i^{obs} - sM(s)_i^{calc})^2/\Sigma_i W_i(sM(s)_i^{obs})^2\}^{1/2}$ is 0.039 where W_i is a diagonal element of the weight matrix. [b]r_i and θ_i denote independent parameters. [c]Dependent on r_i or θ_i. [d]Depentent on C3N1C2C4. [e]Fixed at the B3LYP/6-311++G(2df,p) values.

Figure captions

Fig. 1. Molecular model of diethylmethylamine. The letters t, g^+ and g^- are used to indicate that dihedral angles C4C2N1C3 and C5C3N1C2 are approximately 180, 60 and –60°, respectively.

Fig. 2. Experimental molecular scattering intensities (dots) and theoretical ones (solid lines) of diethylmethylamine with the composition of 35% tt + 27% g^+t + 20% g^-t + 18% g^+g^+; $\Delta sM(s) = sM(s)^{obs} - sM(s)^{calc}$.

Fig. 3. Experimental radial distribution curve of diethylmethylamine; $\Delta f(r) = f(r)^{exp} - f(r)^{theor}$. The pairs listed in Table 4 are indicated by vertical bars. The difference curves $\Delta f(r)$ between the experimental curve and curves calculated by assuming that one conformer exists with its abundance of 100% are also shown.

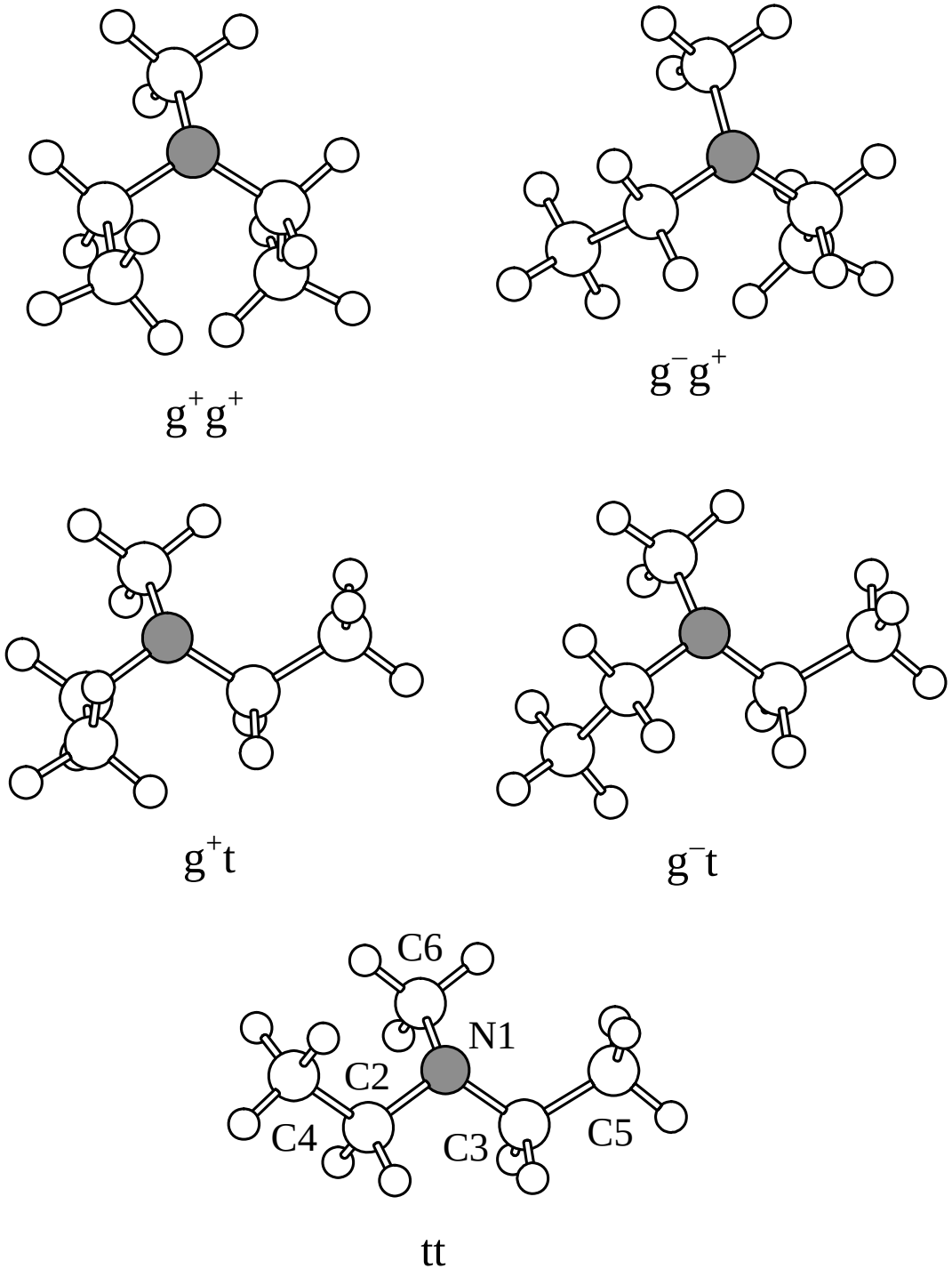

Fig. 1. Takeuchi et al., Molecular structure and conformation of diethylmethylamine determined by gas electron diffraction and vibrational spectroscopy combined with theoretical calculations

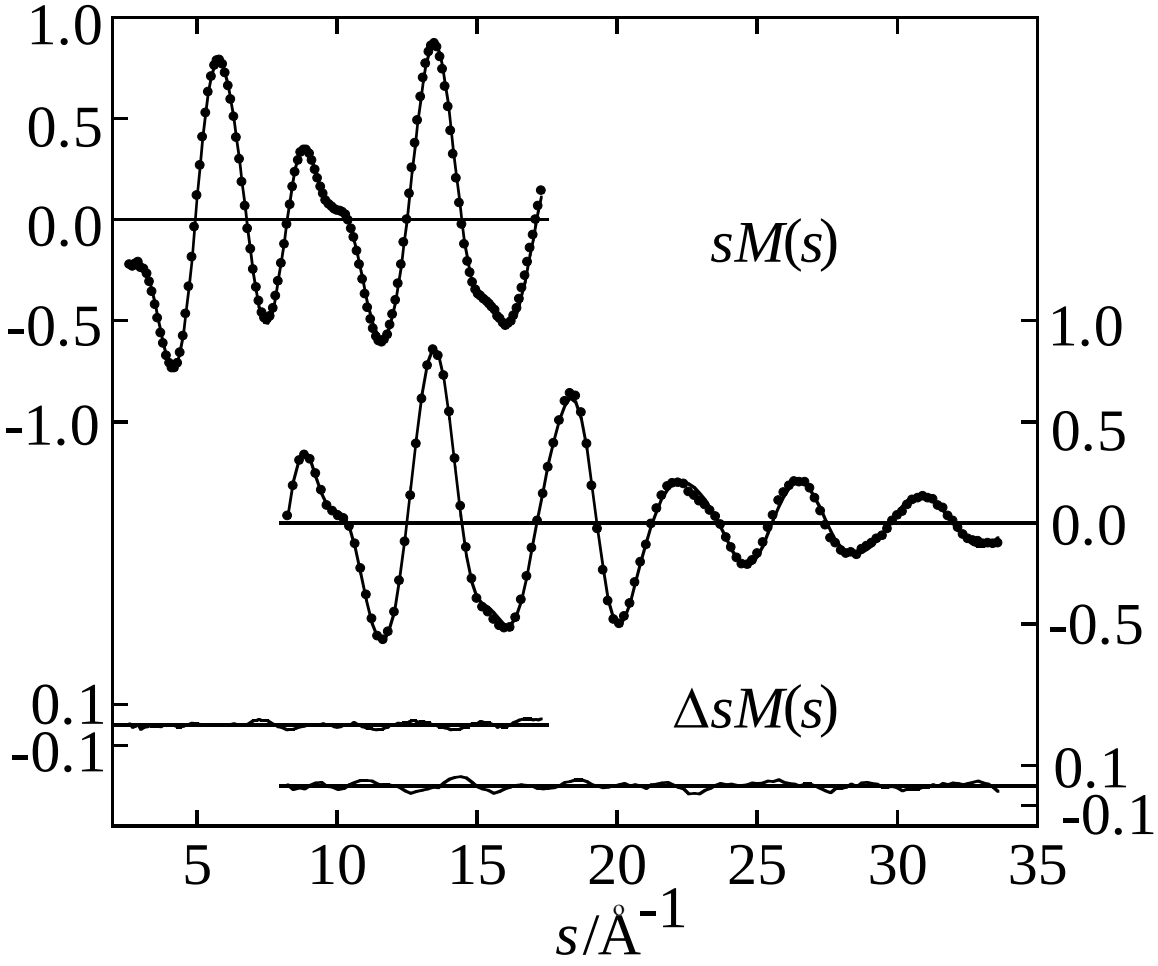

Fig. 2. Takeuchi et al., Molecular structure and conformation of diethylmethylamine determined by gas electron diffraction and vibrational spectroscopy combined with theoretical calculations

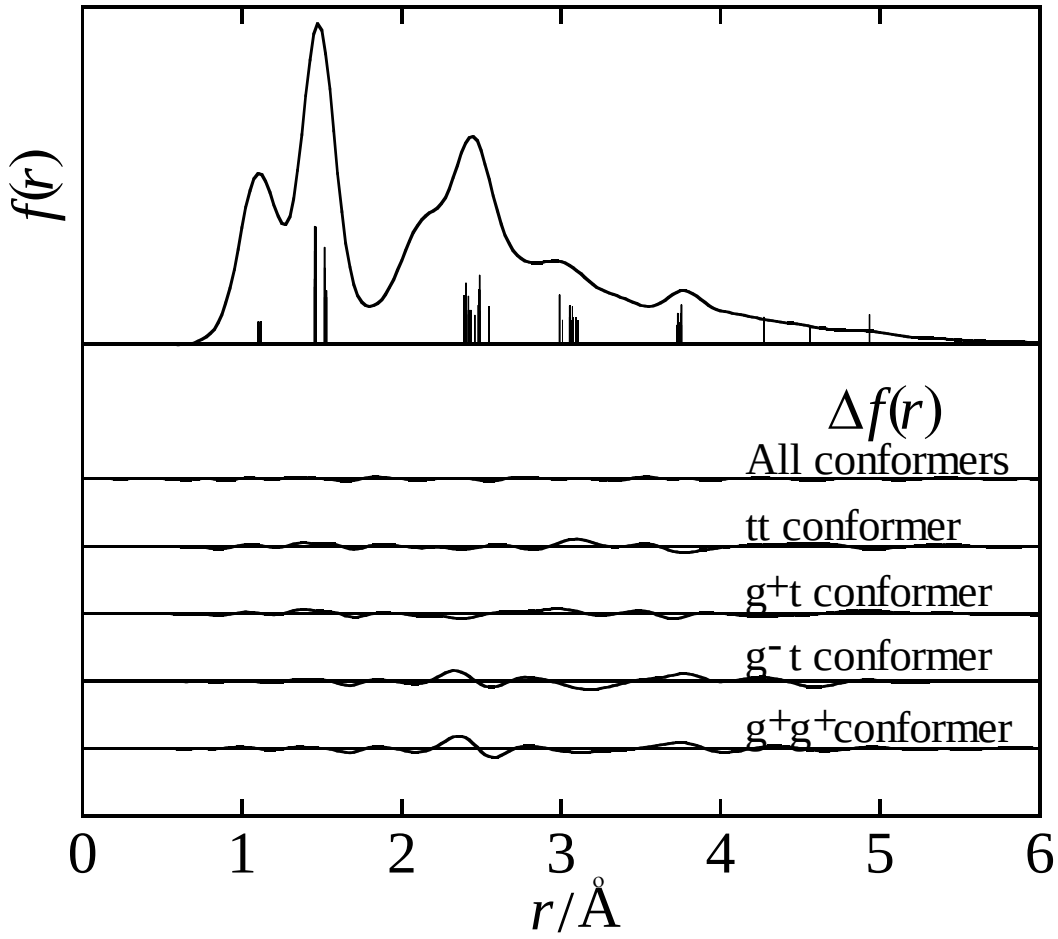

Fig. 3. Takeuchi et al., Molecular structure and conformation of diethylmethylamine determined by gas electron diffraction and vibrational spectroscopy combined with theoretical calculations